Soft Matter

TUTORIAL REVIEW

View Article Online
View Journal | View Issue

Cite this: *Soft Matter*, 2026, **22**, 2597

The hidden wheel-within

Falko Ziebert [ab] and Igor M. Kulić [*c]

Received 13th October 2025,
Accepted 26th January 2026

DOI: 10.1039/d5sm01041a

rsc.li/soft-matter-journal

There is this old, eternal question: Why don't animals have wheels? In this perspective, we show that they actually do, and they do so in a physically extraordinary way – by combining incompatible elasticity, differential geometry and dissipative self-organization. Nature's wheel – the "wheel-within" – has been mysteriously concealed in plain sight, yet it spins in virtually every slender-body organism: in falling cats, crocodilians spinning to subdue their prey, rolling fruit-fly larvae, circumnutating plants and even in some of our own body movements. Flying somehow under the radar of our cognition, in recent years, the wheel-within also tacitly entered the field of soft robotics, finally opening our eyes to its ubiquitous role in Nature. We here identify its underlying physical ingredients, namely the existence of a neutrally stable, shape-invariant and actively driven elastic mode. We then reflect on various man-made realizations of the wheel-within and outline where it could be spinning from here.

The wheel and axle, as pinnacles of early human technology, are still at the core of many of our mechanical devices. In an abstract sense, the wheel–axle system is an object exhibiting a single, cyclic degree of freedom that in spite of its internal rearrangement keeps its outer shape constant, *i.e.*, it moves within its "own skin". This "iso-skinning" feature is exceptionally useful as the wheel–axle can be placed within fixed shape enclosures and combined predictably with other elements. Since the earliest days of biology, people have wondered whether the wheel–axle principle was discovered during evolution and, if not, why so. The usual suspects for the wheel's (apparent) absence range from its impracticability in the absence of high quality roads to its difficult discoverability by small mutations – Nature being unable to overcome "Mount Improbable".[1] These are some of the echoing thoughts of self-confident (technological) teenagers – us, the humanity – reflecting about the seeming shortcomings of their parent. Could there be something we are missing here? It might come as a surprise that Nature found its own version – and in fact a technologically superior generalization – of a "cyclic isoskinning" device: the wheel-within.

Recent work[2,3] describes a peculiar motion of fruit fly larvae on surfaces. The larva bends its body into a half-doughnut shape and, by contracting its circumferential body muscles in a cyclic manner, generates a rotation around the curved body axis to finally engage in a rolling-like mono-wheel propulsion. The seemingly quirky curiosity turns out to be only one instance of something much more universal, which we coin Nature's wheel-within. A much earlier encounter dates back to James C. Maxwell, who repeatedly threw his cat from a (ground floor) window and began wondering how it always lands safely "with its feet down".[4] It took a century of scientific debate to realize that – similar to the larva – during the fall, the cat body forms a half-doughnut and *via* differential muscle contraction manages to reorient its feet downwards.[5–8]

In the following, after familiarizing us with more examples from Nature, *cf.* Fig. 1, we will dissect what they all have in common. We identify the three main physical ingredients of this unexpected motion: first, the existence of a neutraly stable or zero-elastic energy mode; second, the shape-invariance or "iso-skin" property of this mode in analogy to a wheel; and finally a suitable, dissipative or active, coordinated or self-organized driving process of this mode, with the principle of "incompatible equilibria" or "dynamic frustration" being an especially efficient realization. After explaining the concept, we review the many – sometimes only partial – realizations of the wheel-within in soft robotics for variously shaped actuators and motors. We classify the different occurrences of the wheel-within concerning their degrees of freedom and number of "wheel-modes". Finally, we outline possible future directions and unravel the hidden possibilities of the wheel-within.

[a] *Institute for Theoretical Physics, Heidelberg University, Philosophenweg 19, 69120, Heidelberg, Germany*
[b] *BioQuant, Heidelberg University, Im Neuenheimer Feld 267, 69120, Heidelberg, Germany*
[c] *Institut Charles Sadron UPR22-CNRS, 67034, Strasbourg, France. E-mail: kulic@unistra.fr*

The wheel-within in nature

Reflecting on the motion of fruitfly larvae and cats as shown in Fig. 1, one quickly realizes a general motif behind: the one of a

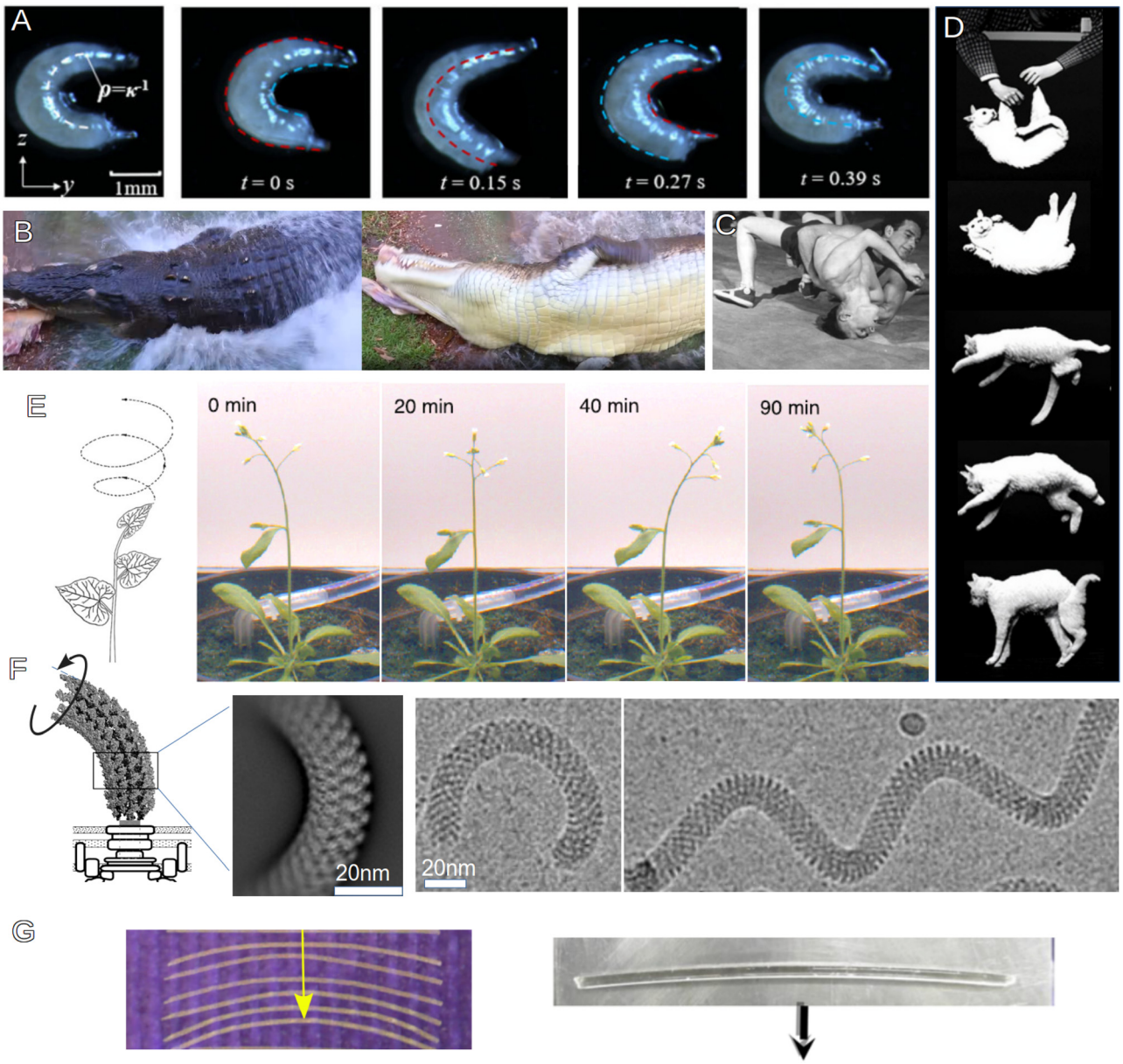

Fig. 1 The "wheel-within" is a universal tool of Nature and utilized by many slender organisms in fauna and flora: (A) A Drosophila larva rolling on a substrate reproduced with permission,[3] copyright 2025 American Physical Society. (B) A crocodile's death roll when catching a prey.[9] Snapshots from "ELVIS THE CROCODILE DEATH ROLL", Australian Reptile Park, Youtube, https://youtu.be/1sqw49cQWOo (accessed Aug 11 2025). (C) A wrestler performing the "bridge", also called "upa" in Brazilian jiu-jitsu.[10] Allgemeiner Deutscher Nachrichtendienst, Bild 183-33533-0005: CC-BY-SA 3.0. (D) A falling cat, spinning around to land on the feet. Enhanced and modified from É. J. Marey, Falling Cat 1894 (Public domain). (E) Circumnutation, *i.e.* spinning around the gravity axis during growth, of *Arabidopsis thaliana* modified with permission,[11,12] copyright 2020 Elsevier. (F) The flagellar hook: the left panel shows a sketch of the hook on top of the rotary motor; the other panels show cryo-EM pictures. Modified with permission,[13] copyright 2019 Springer Nature. (G) Two artificial, self-organized wheels-within ("fiberboids"): on the left a stroboscopic image of a spaghetti driven by osmosis to roll on a humidified kitchen towel, on the right a thermally driven PDMS fiber rolling on a hot substrate.[14,15] Fiber length is 6 cm (left panel) and 11 cm (right panel).

slender object, whose cross-sections contract circumferentially, keeping the overall shape (roughly) invariant. This motif is found across scales and all over the plant and animal realm: similar motion can be observed on the macroscale, for instance, crocodiles spinning in the water after having caught their prey – the so-called "crocodile's death roll"[16] – or in human pole jumpers or wrestlers. Examples from the micro- and nanometric scale include microswimmers such as spirochetes[17,18] (the causative agent of Lyme's disease), as well as the rotary-motor-driven shape-invariant spinning of the bacterial flagellar hook.[13,19,20] In the plant realm, the wheel-within hides in a process called "circumnutation" – a phenomenon already described by Charles Darwin:[21] the spinning of a growing plant around the gravity axis due to radially asymmetric osmotic swelling and growth rates.[11,12]

Table 1 Examples from Nature. The ZEEM can be emergent (*i.e.*, the curvature is created concomitantly) or intrinsic. The number of degrees of freedom (DoFs) in the emergent cases, as well as in plants, is two, since not only the orientation of curvature but also its absolute value are variable. The flagellar hook has only one degree of freedom. The other rows discuss the driving mechanism, whether the motion is self-organized or externally driven, and what the motion is typically used for. All examples have (albeit some having only approximately) the isoskinning property

System (Nature)	ZEEM	Number of DoFs	Origin of the drive	Type of drive	Effect/use
Cat[4]/crocodile[16]/wrestler	Emergent	2	Neuromuscular	Internal	Reorientation in 3D
Rolling larvae[2,3]	Emergent	2	Neuromuscular	Internal	Rolling + translation
Spirochete[17,18]	Emergent	2	Molecular motors	Internal	Swimming
Circumnutating plant[21]	Intrinsic	2	Dynamic osmotic stress	Internal	Translation + rotation
Bacterial flagellar hook[13,19,20]	Intrinsic	1	Rotary motor	External	Torque transmission

Some of these examples are illustrated in Fig. 1. The wheel-within enables Earth's flora and fauna to perform various tasks: to roll on rigid substrates (larvae), to swim through viscous fluids (spirochetes) and even to inertially reorient in "empty space" (falling cat) and as a clever means to transmit torque around a corner (flagellar hook), see Table 1. Different – and somewhat unrelated – explanations have been put forward for each of these phenomena. In the physics literature, the cat-spinning was treated in the abstract framework of geometric phases and an-holonomy,[22] with the notable exception of a short note by Lecornu[23] already identifying the cat with a spinning torus. Plant circumnutation was rationalized with mechanical models coupled to growth.[11] In view of the striking commonalities, however, it becomes pertinent to identify the unifying concepts that could serve as a framework transferable to man-made machines.

Initially unaware of Nature's wheel within, some time ago we created a family of peculiar elasto-dynamic engines – the toroidal "fiberdrive"[15] and its open (*i.e.*, not closed to a torus) fiber analogue, the "fiber-boid".[14] Fiberboids, see Fig. 1G, are macroscopic polymeric fibers with a circular cross-section that when placed on a surface subject to an energy–matter flux (*e.g.*, a thermal or humidity gradient) start to roll along the surface. The fiberdrive, in turn, is a fiberboid closed to a torus, see Fig. 2A and 3B, that if driven rotates in the poloidal direction (*i.e.*, every cross-section turns around the centerline). Playing with these strangely counterintuitive minimalistic engines, and at the same time seeing the rolling larvae, strangely resonates and after some thought strongly suggests that one is seeing instances of the same shape-invariant kinematics and dynamics.

Active, neutrally elastic, isoskinning modes

So, what are the main physical ingredients for the wheel-within to run? First, there is the existence of a neutrally stable mode, or zero-elastic energy mode (ZEEM). In many physical systems, it is a common phenomenon that bi- or multi-stability occurs, meaning the system displays several energy minima. Note that in elastic systems, such minima typically imply different shapes. If in addition these minima lie continuously along a curve at equal energy, one calls the system elastically "neutrally stable". As a consequence, it costs no energy to move along this path, implying in turn a continuous deformation mode at no energy cost. Because there is (in the idealized case) no resistance to an applied force, in mechanical engineering, such elastic systems are also called "zero-stiffness structures",[27] exhibiting a ZEEM.[15]

Some example structures are shown in Fig. 2A–C. Fig. 2A shows the fiberdrive, a torus displaying a "circular ZEEM":[15] rotating a cross-section in the poloidal direction does not cost energy. The underlying reason is that, due to the topological constraint of the torus shape, the absolute value of the (centerline) curvature is fixed, but its orientation with respect to a cross-section is free and constitutes a zero-elastic energy mode. Fiberboids[14,15] – open fibers – can be considered as parts of a torus with their curvature being induced by the same energy–matter flux that drives them. Other examples include bilayered shells, *cf.* Fig. 2B, as well as edge-crumpled sheets and several variants of Möbius strips. A very illustrative example for a ZEEM is shown in Fig. 2C and was introduced in ref. 25 and 26. The structure is an arc-shaped shell, where an inflection point can be moved freely along a one-dimensional neutrally stable path, since the energy is constant (see the sketch) except at the "ends", where it decreases as the structure prefers a shape without an inflection point there. While the other examples

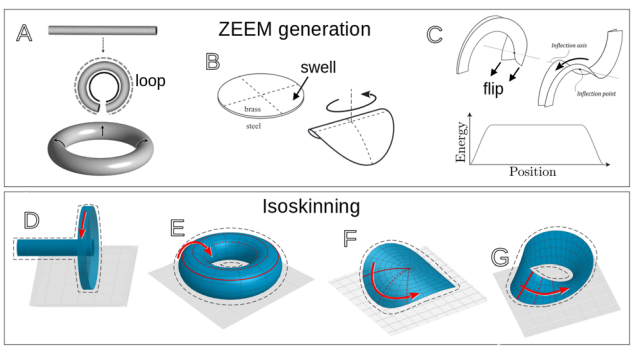

Fig. 2 (A)–(C) Neutrally stable/zero-elastic energy modes (ZEEM). (D)–(G) Isoskinning objects with neutral modes. (A) A torus formed by bending a rod and glueing the ends together as the simplest structure displaying a circular ZEEM.[15] (B) Shell structure made of two different layers.[24] (C) Neutrally stable mode in a "kinked" arc-shaped shell:[25,26] the inflection point can be moved along the crest without energy cost (see the flat energy region in the sketch below). (D) The rigid wheel–axle system: the wheel turns (red arrow) round the axle while keeping the outer skin (dashed) invariant. (E) A neutrally stable torus rotating around its curved centerline. (F) A neutrally stable self-buckled shell reorienting by keeping its outer skin fixed. (G) A neutrally stable twist deformation of a Möbius strip moving along its center-line within the same skin.

display circular ZEEMs, as required for a wheel, the last example is a ''translational ZEEM''.

Inspecting the examples from Nature again, there the ZEEM is intrinsic for circumnutating plants (gravity buckling) and the bacterial flagellar hook (incompatible strains), but it can also be emergent, *i.e.*, self-organized under intrinsic forces, as in the spinning cat and spirochetes, *cf.* Table 1. All examples from Nature, except the flagellar hook, have two degrees of freedom: the one associated to the ZEEM (the rotation around the curvature centerline) and the absolute value of the curvature (which will be identified later as a ''modulator mode'', see Fig. 5). In that sense, the examples from Nature correspond most closely to the fiberboid (Fig. 1G), with most other man-made examples so far (torus, Möbius strip, *etc.*) having only one degree of freedom (see later and Fig. 5).

Box 1: Driving the wheel-within: piston–crankshaft analogy.

As explained in Fig. 3, the fiberdrive has a formal analogy with a piston engine. We consider here a toy model of 4 sub-fibers (''pistons'') arranged at 90° orientations running at constant distances across each cross-section around the torus. They will be referred to as pistons, since their length changes coupled with the fiber geometry lead to a collective rotation of the whole device, the fiber geometry itself acting as an equivalent of the crankshaft by enslaving the pistons to share a common orientation angle $\Phi(t)$ of the cross-section with respect to the outer frame. Each piston fiber ($k = 0,\ldots,3$) is characterized *via*
(a) the time-dependent temperature $T_k(t)$, implying *via* an equation of state their mechanically preferred piston extensions $x_k(t)$,
(b) the thermodynamically preferred piston temperatures

$$T_k^{\mathrm{ext}}(\Phi) = \bar{T}\left(1 + a_{\mathrm{T}}\cos\left(\Phi + k\frac{\pi}{2}\right)\right), \tag{1}$$

as set by the external baths and characterized by the mean temperature $\bar{T}$ and $\Delta T_{\mathrm{ext}}^{\varepsilon} = 2\bar{T}a_{\mathrm{T}}$ its variation in z-direction, perpendicular to the torus plane, and
(c) the *mechanically imposed* piston extensions

$$X_{\mathrm{k}}(\Phi) = L\left(1 + a_{\mathrm{X}}\sin\left(\Phi + k\frac{\pi}{2}\right)\right), \tag{2}$$

as enforced by the action of the crankshaft geometry, where $L = 2\pi/\kappa$ is the centerline length of the closed torus with a (large-circle) curvature κ. This curvature and the imposed piston extension are related *via* the strain $\varepsilon = \frac{La_{\mathrm{X}}}{L} \simeq \kappa a$, where a is the (poloidal) radius of the torus – also assumed to coincide with the lateral size of the pistons.

Note that both (1) and (2) are explicit functions of a single collective variable – the angle Φ. They both are constrained by the geometry of the device and their mismatch (here a 90° phase shift, *cf.* cos *vs.* sin) together with the inability of the system to match both is exactly what drives the engine.

There are two types of dynamic relaxation processes, a thermodynamic and a mechanical one. The thermodynamic relaxation dynamics is given by Newton's law of cooling

$$\dot{T}_{\mathrm{k}}(\Phi,t) = \gamma(T_{\mathrm{k}}^{\mathrm{ext}}(\Phi) - T_{\mathrm{k}}(t)), \tag{3}$$

where we assume that the pistons can be seen as having a uniform temperature.† γ is a relaxation rate and its inverse $\tau = \frac{1}{\gamma}$ represents the typical thermal relaxation time for the pistons to equilibrate with their environment.

The temperature of the pistons and their extensions result in a force that originates from the equation of state specific to the piston material. We assume the simplest expansion of the free energy for small temperature and length changes:

$$\mathcal{F}(T,X) \approx \mathcal{F}_0(T) + \frac{YLa^2}{2}\left(\alpha(\bar{T}-T) - \frac{L-X}{L}\right)^2.$$

Apart from an extension independent part, it has a linearly elastic part that couples the thermal prestrain with the actually realized strain. The thermal prestrain depends on the thermal expansion coefficient α and the temperature difference to the reference temperature, $\bar{T}$, corresponding to vanishing prestrain. The Young's modulus Y is assumed to be temperature independent. Differentiating the free energy with respect to the piston extension yields the piston force:

$$f_{\mathrm{k}}(\Phi,t) = Ya^2\left(\frac{L - X_{\mathrm{k}}(\Phi)}{L} - \alpha(\bar{T} - T_{\mathrm{k}}(t))\right). \tag{4}$$

Noting that the crankshaft constrains the system to only a single degree of freedom, the collective angle Φ, we can write down a Lagrangian:

$$\mathcal{L}(\Phi,\dot{\Phi}) = \sum_{k=0}^{3} f_{\mathrm{k}}X_{\mathrm{k}}(\Phi) + \Phi M_{\mathrm{ext}} + \frac{I}{2}\dot{\Phi}^2$$

where the first term describes the potential energy (of piston extensions), the second term the effect of a possible external torque and the last term rotational kinetic energy (with I the effective moment of inertia), which will be neglected in the following for slow turning. Forces originating from mechanical dissipation, *i.e.*, friction, can be accounted for by introducing the Rayleigh dissipation functional $\mathcal{R} = \frac{1}{2}\xi\dot{\Phi}^2$. The mechanical force balance, given by the Rayleigh–Lagrange dynamics,

$$\frac{\partial\mathcal{L}}{\partial\Phi} - \frac{\mathrm{d}}{\mathrm{d}t}\frac{\partial\mathcal{L}}{\partial\dot{\Phi}} = \frac{\partial\mathcal{R}}{\partial\dot{\Phi}},$$

then yields

$$\sum_{k=0}^{3}\left[f_{\mathrm{k}}\frac{\partial X_{\mathrm{k}}}{\partial\Phi} + \frac{\partial f_{\mathrm{k}}}{\partial\Phi}X_{\mathrm{k}}\right] + M_{\mathrm{ext}} = \xi\dot{\Phi}. \tag{5}$$

Eqn (1)–(5) are easy to solve in the steady state by replacing $\Phi \to \omega t$ with a finite angular velocity ω and using an ansatz

$$T_k(t) = T_0 + T\cos\left(\omega t + \theta + k\frac{\pi}{2}\right), \tag{6}$$

with a to-be-determined phase angle θ.
The resulting motor-relation (torque–angular velocity relation) reads

$$\left(\frac{\omega^2}{\gamma^2} + 1\right)(\xi\omega - M_{ext}) = M_{drive}. \tag{7}$$

The driving torque is given by

$$M_{drive} = (La^3)Y\kappa(\alpha\Delta T^{\varepsilon}_{ext}) \tag{8}$$

and has a simple interpretation: up to a geometrical factor, it is given by the stiffness, the geometry-imposed curvature and the thermal expansion-induced driving strain. For a small drive (and no external torque), the angular velocity is simply given by $\omega = \frac{M_{drive}}{\xi}$ and the phase angle amounts to $\theta = -\frac{\omega}{\gamma}$.

The second major ingredient for the wheel-within to work is the isoskinning (or Iso-surface) property: to be a true wheel-within, the motion of the body must keep its enclosure's surface (its "skin") invariant, see Fig. 2D–G. Of course, in Nature – thinking of the cat – this may just be approximately realized. The simplest example is obviously the classical, man-made, rigid wheel, Fig. 2D. The most elegant wheel-within is probably the torus-shaped fiberdrive,[15] see Fig. 2E, where every cross-section rotating at a constant speed leaves the whole object shape-invariant. More examples include bent sheets, see Fig. 2F, realized in ref. 28, as well as Möbius strips, see Fig. 2G, realized in ref. 29–31 (see also Fig. 4 for more examples of man-made realizations). In all the sketches of Fig. 2D–G, the dashed curve describes the invariant "skin" of the object and the red arrow indicates the ZEEM direction.

More precisely, we define isoskinning as "a surface-preserving body transformation *modulo* Euclidean space motion (3D translation and rotation)". This makes it different from an isometry, since for isoskinning, there can be local contractions/dilations which change the metric of the surface (and the bulk as well). Another example that still is isoskinning is the falling cat, where a counter-rotation of the skin itself exists to conserve the total angular momentum – in fact, this "skin rotation" is the very purpose for the cat using the wheel-within, to land on its feet.[5–8] An example where isoskinning is only partially fulfilled is circumnutation in plants: while the contribution of osmotic water redistribution is isoskinning, the contribution from cell growth is not, making isoskinning only approximately valid along the longitudinal direction.

The third and last ingredient of the wheel-within is an active drive: to make the wheel turn, the neutral mode having the isoskinning property has to be driven by a nonequilibrium process coupled to elastic stresses and strains. Many different driving mechanisms appear possible and some of Nature's realizations include active (ATP-consuming) muscle contraction in the animal realm, *cf.* Fig. 3A, or osmotic stresses in plants. For man-made systems, a temperature difference/heat flux can be used as in the fiberdrive,[15] a polymeric macroscopic torus heated from below, as shown in Fig. 3B and with the mechanism detailed in Box 1. Other examples include hygroscopic (de)swelling,[14,32] *i.e.*, a solvent enters/leaves a network-based material, or light. The latter can drive the ZEEM either indirectly *via* local heating,[33,34] or directly, *e.g.*, *via cis-trans*-isomerization of light-sensitive molecules like azobenzene that are embedded in a matrix.[35]

In spite of this plethora of possible driving mechanisms, there is a serious catch that whoever practically tries to

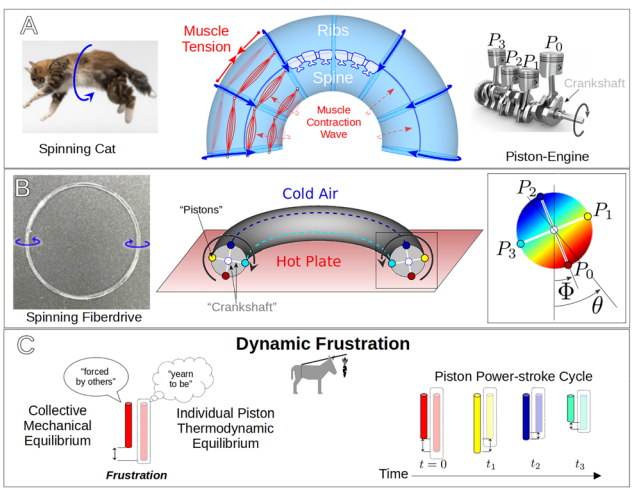

Fig. 3 Active driving, crankshaft analogy and dynamic frustration. (A) A falling cat, spinning to get on its feet, seen as part of a torus. The analogy to the piston engine: the spine/ribs correspond to the crankshaft and the contractile muscles (which are actuated by the animal) to the pistons. (B) In the fiberdrive, a closed torus heated from below, one can consider parts of material, *e.g.*, as indicated, as the pistons. The crankshaft arises due to the material's connectivity. (C) Dynamic frustration/incompatibility of equilibria: every piston has a current length (left) that differs from its thermodynamically preferred length (right) at the given temperature. This leads to a situation where every piston is "frustrated", creating an overall torque.

† This is the case for small Biot number $\mathrm{Bi} = ha/k_p \ll 1$, where h is the heat transfer coefficient, k_p the piston's thermal conductivity and a its diameter. The relaxation rate γ can then be expressed in terms of the specific heat capacity c_p, the mass of the piston m_p and the effective area aL for heat exchange as $\gamma = \frac{haL}{m_p c_p}$.

induce the isoskinning motion along a ZEEM quickly can confirm: not all types of non-equilibrium stress generation will induce the desired motion. In fact, most will do nothing at best, merely deforming and, more often than not, irreversibly destroying the sample. However, there is a systematic solution for efficient driving: the principle of ''incompatible equilibria'' resulting in a steady state of ''dynamic frustration''.

Incompatible equilibria and dynamic frustration

Rotation of the wheel-within needs some form of highly coordinated, geometrically orchestrated generation of stresses and strains that couple out of phase to generate torques. That is where a phenomenon that we might call dynamic frustration comes into the game.

To illustrate the concept intuitively, we may remark that many of the biological and man-made examples can be understood by thinking of a rotary piston-engine, see Fig. 3 and Box 1, with their pistons performing thermodynamic power-stroke cycles. Much like in a car engine, the pistons are not independent but rather rigidly coupled *via* some form of constraint that we might call the ''crankshaft'' in analogy to classical engines. In a falling cat, *cf.* Fig. 3A, the crankshaft is constituted of the cat's incompressible spine, together with its radial rib-skeleton connecting up to the muscles which act as the pistons. In the toroidal fiberdrive, *cf.* Fig. 3B, the crankshaft is emulated by approximate mechanical constraints of the cross-section's circularity and the centerline incompressibility. This virtual crankshaft enslaves the contracting pistons – the longitudinal muscles or the actuating material sections – to share one or two common degrees of freedom, forcing them to synchronize their action. An idealized cat has two degrees of freedom, the amplitude and the phase angle of its body curvature, while a toroidal fiberdrive has only one degree of freedom (the phase), since the magnitude of the curvature is rigidly maintained by the closure constraint of the torus. The fiberboids, linear rolling fibers, can be viewed as parts of a torus and are the analogue of the cat in the sense that they have again two degrees of freedom, phase and magnitude of curvature, the latter emerging from the dissipative coupling of the fiber with the planar substrate. In Box 1 and Fig. 3C, we explain a simple one-dimensional version of the fiberdrive, based on 4 coupled pistons, in more detail, including the specific driving mechanism, the equation of state that couples the drive to the pistons, and the resulting (steady-state) dynamics.

Importantly, beyond the coupling *via* the ''crankshaft'', rotary motion needs a phase shift of the thermodynamic and mechanical equilibrium positions, which induces what we call ''dynamic frustration''. For the fiberdrive, a torus lying on a hot plate, the phase shift is 90°: the geometry induces in-plane strains (due to the torus' curvature) while the thermal gradient induces (thermal expansion) strains in the direction normal to the plane. Other phase shift values are of course possible but typically less efficient.‡ Importantly, this phase shift renders the two equilibria – thermodynamic *vs.* mechanical – mutually incompatible. This incompatibility can hence be purposefully introduced to prevent the existence of any static equilibria, enforcing a constant state of motion of the system, much like the allegorical donkey that perpetually chases a carrot attached *via* a rigid pole to its back.

Finally, a more subtle point is the relation between the thermodynamic and mechanical variables, which closes the system in the physical sense. In a purely physical system, this is simply the piston's equation of state (*cf.* Box 1), which relates temperature – or chemical composition, *etc.*, depending on the specific drive – to its length and generated force. In biological systems, like the spinning cat or rolling larvae, this closure relation is more complex and sometimes difficult to specify. For the cat, it results from neuromuscular feedback closely related to the organism's ability to perceive its own body shape and space orientation and to dynamically steer muscle tension in accordance with them, in order to reach the goal of the created motion, landing on its feet.

Man-made wheel-within

Without noticing its natural existence and fully grasping its unifying concept, the wheel-within recently entered our technology. Examples are shown in Fig. 4, and Table 2 provides a rough classification. As our focus lies on the physical principles, we do not give an exhaustive review here and refer to ref. 39 for an overview of realizations of the wheel-within from the materials science point of view – focusing on liquid crystalline elastomers (LCEs) as especially versatile materials – and to ref. 40 for a review from the viewpoint of autonomous robotics.

Starting with the torus geometry, it was introduced using basic polymeric materials (nylon and PDMS), on the macroscopic scale (cm sized) and with thermal drive (heating plate) in ref. 15. The geometry can be modified, *e.g.*, to twisted rings[41] and to Archimedean spirals,[15] see Fig. 4C. The latter can be regarded as several concentric tori put in series, allowing to add up and hence magnify the created torque. More importantly, the driving mechanism was replaced by light (photothermal)[34,42] and the object could be miniaturized. Several interesting modes of motion can be achieved with tori, including translational motion,[15] swimming in a viscous fluid, as shown in Fig. 4A, and moving along guiding tracks, including fibers and interior walls of micro-pipettes.[34]

There is a plethora of examples for fibers, see also ref. 39. Interesting early work on a macroscopic PDMS cylinder exists, where a droplet of solvent was placed on one side, inducing hygroscopic swelling and transient uphill rolling.[32,43] Though the motion was not yet perfectly self-sustained, some elements

‡ For a zero phase shift, there is no torque and for a phase shift of π, stress is proportional to negative strain, *i.e.*, one has a local (unstable) equilibrium with again zero torque. The optimum phase shift of stress and strain is reached somewhere between these two extreme values.

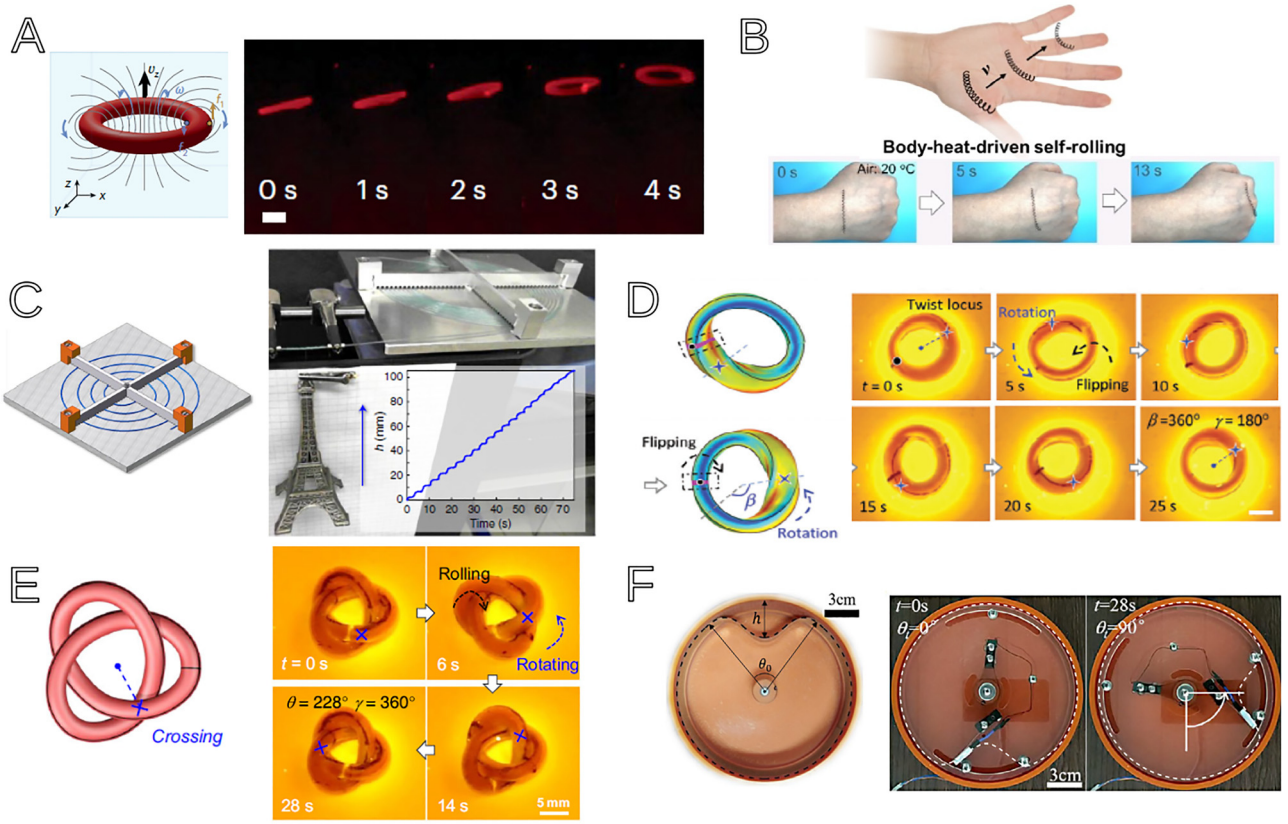

Fig. 4 Man-made examples of the wheel-within. (A) A photo-thermally driven fiberdrive (torus) swimming in a liquid in the low Reynolds number regime modified from ref. 34 under Creative Commons CC BY license, Springer Nature (2024). (B) A (helical) fiberboid utilizing body heat to roll along a human arm modified with permission,[36] copyright 2024 John Wiley and Sons. The helical shape slightly breaks the perfect ZEEM, but also has advantages like a better adaptation to the surrounding. (C) An Archimedean spiral can be seen as several fiberdrives mounted in series, adding up the torques they can exert to lift a weight.[15] (D) A Möbius strip made of a composite material (anisotropic hydrogel with plasmonic nanoparticles) that rotates under static light illumination modified with permission,[30] copyright 2024 John Wiley and Sons. (E) A "knotbot", performing two modes of motion: poloidal ("rolling") and toroidal ("rotating") under static light illumination. Modified from ref. 37 under Creative Commons CC BY license, Springer Nature (2024). (F) A confined blister that rotates when heated along its circumference; modified from ref. 38 under Creative Commons CC BY license, John Wiley and Sons (2024).

Table 2 Man-made examples. A table analogous to Table 1 for man-made examples, discussing whether the ZEEM is emergent or hard-coded in the geometry/topology, the number of degrees of freedom (DoFs), the driving mechanism and what the motion can be used for. In addition, all examples in the table are isoskinning

System (manmade)	ZEEM	Number of DoFs	Origin of the drive	Effect/use
Torus (fiberdrive)[15,34,42]	Intrinsic	1	Thermal,[15] photothermal[34]	Torque transmission, swimming, track-based motion
Spiral[15]	Intrinsic	1	Thermal	Torque generation
Fibers (fiberboids)[14,15,33,35,44]	Emergent	2 (1 ZEEM + 1 modulator)	Thermal,[14,15,44] hygroscopic,[14] photothermal,[33] photomechanical[35]	Rolling, translation, robotic tasks
Möbius/Seifert strips[30,49]	Intrinsic	1	Photothermal	Spinning, track-based motion
Knots[37]	Intrinsic	2 (2 ZEEMs)	Photothermal	Spinning, track-based motion
Sheet,[28] blister[38]	Intrinsic	1	Thermal	Spinning, fluid pumping

of shape invariance and "dynamic frustration" emerged there, foreshadowing the following developments. Self-rolling started with ref. 14, 15 and 44 using very basic polymeric materials, while nowadays advanced materials have been designed, including as examples light- or thermally powered mono-domain LCE rods[33] and light-driven core–shell fibers.[45] Multiple modes of motion have been described on different substrates[46] and twisted/helical fibers have been created.[47] The latter can even roll on a human arm, utilizing just body heat,[36] see Fig. 4B, and helical fibers have been designed to fulfill basic robotic tasks and navigate in a 2D maze.[48] Finally, since photothermal activation is often prone to damaging the material, direct (*i.e.*, not photothermal) light activation using photoswitchable azobenzene was achieved as well.[35]

The Möbius strip geometry also allows for ZEEMs, see Fig. 4D, and several variants, typically photothermally driven,

have been realized.[29–31,49] First the light source had to be focused on the locus of the twist regions and hence had to be continuously moved[29] – the cooling time of the material was too long and thermal damage prevented ''dynamic frustration''. Later on, activation by continuous radiation was achieved, first for LCE-based Seifert ribbons.[49] Using PNIPAm-based hydrogels with embedded nanosheets (for anisotropic response) and gold nanoparticles (for light absorption), finally, Möbius strips[30] were realized that rotate under continuous radiation, profiting from self-shadowing effects followed by new exposure to light when turning.

A very interesting geometry class with a novel effect is the so-called ''knotbot'',[37] *i.e.*, a closed knotted filament as shown in Fig. 4E. It displays not only the poloidal ZEEM, similar to the simple (unknotted) torus, but also a second ZEEM: a toroidal motion along the circumference, to which we will come back below.

Finally, actuated sheet geometries have been proposed, like the kinked arc-shaped sheet,[25] *cf.* Fig. 2C, which was recently also thermally driven.[26] Although this example lacks the isoskinning property, it still appears very appealing for robotic actuation. Neutrally stable modes have been shown to exist in several other slender 2D objects like prestressed shells and sheets[24,27,50,51] and some of these modes were actively driven.[28,52] A nice example of a true isoskinning ZEEM was achieved by confining a sheet in a cylindrical enclosure, yielding a rotating blister,[38] see Fig. 4F.

To classify the plethora of geometries proposed so far, it is important to note that the ZEEMs occurring in the so far created man-made examples are all intrinsic: they are built-in either topologically (*e.g.*, in the torus, the Möbius strips and the knotbots) or set by other constraints (spinning spiral and bulged sheets) or incompatible stresses (for crumpled sheets). The only exception seems to be the self-rolling fiber – and the examples from Nature: here the active, neutrally elastic, isoskinning mode is spontaneously emerging (bifurcating) from the cylindrically symmetric object in the absence of the drive.

Another interesting classification relates to the number of ZEEMs, see Fig. 5: the torus has the poloidal ZEEM that was our main focus so far, while the Möbius-like strips have a single toroidal ZEEM, *cf.* Fig. 5A. The crumpled sheet and the fiber geometry also have only one ZEEM, but now this mode can be modulated, see Fig. 5B: the amplitude of the crumpled rim and the curvature of the fiber, respectively, depend on the amount of drive. This ''modulator mode'' makes the fiber geometry so versatile that it can adapt to the surrounding and it hence seems not to be a coincidence that the examples from Nature have this modulator mode. As seen in Fig. 4E, the knotbot is again different: it has two ZEEMs, one in the poloidal and one in the toroidal direction, *cf.* Fig. 5C, and hence could be called a ''two-wheel'' to distinguish it from the ''mono-wheels'' discussed so far. Finally, a ''three-wheel'' is also possible theoretically, with one potential realization being a crumpled (*e.g.*, deflated) spherical shell as shown in Fig. 5D. In all these examples, the ZEEMs correspond to modes restoring broken continuous symmetries of the underlying manifolds, with the symmetries being broken either by topological constraints or by bifurcations. In this sense, they can be seen as geometric, actively driven analogues of Goldstone modes.[53,54] Such modes appear in bulk condensed materials whenever a continuous symmetry is broken and correspond to slow (hydrodynamic), low (zero) energy modes with classical examples being the rotation of the magnetization or the nematic director in a ferromagnetic solid or a nematic liquid crystal, respectively.[53] Among the Goldstone modes in solids, the ZEEMs however stand out in that they involve a literal matter-flux along the respective directions. Thus, they can be seen as solids with one (or respectively two or three, see Fig. 5) entrapped fluid mode(s).

Perspectives: where the wheel-within is rolling

By creating artificial wheels-within with colleagues in the field, we unknowingly stepped into Nature's territory, offering a blissful view to the mysterious minimalism and efficiency of the natural wheel-within. It shows no frictional wear between its components, as it has only a single one. It can emerge into and pass away from existence in any slender organism – after

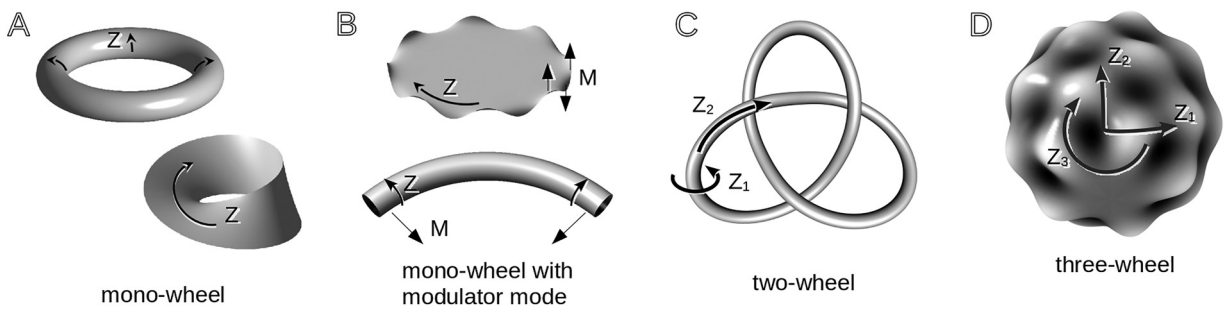

Fig. 5 Degrees of freedom of the wheel-within family. (A) The fiberdrive (torus) and the Möbius strip as ''mono-wheels'' with a single ZEEM (Z). (B) Fiberboids (open fibers) and crumpled sheets have two degrees of freedom: one ZEEM (Z) and one auxiliary bending mode (M) with finite stiffness that can modulate the active dynamics of the ZEEM. All known wheels-within in Nature are of this type, with the exception of the flagellar hook. (C) Any elastic knot (knotbot) has two ZEEMs: a poloidal (Z_1) and a toroidal ZEEM (Z_2). (D) A raspberry-like deflated and crumpled elastic sphere can in principle have three ZEEMs, corresponding to three spatial rotations.

all, a cat has many more things to do than spinning in the air. A snake, for instance, can propagate sinusoidal waves down its body to swim or slither on the ground, it can generate propagating kink pairs to climb trees[55] and it can spin its wheel-within if it needs to. Also, a manta ray can propagate waves along its leaf-like body to thrust forward, or it can create an isoskinning mode to reorient its swimming direction. In this sense, any slender-body organism is a kinematic multi-tool Swiss army knife of evolution. Its emergent wheel-within is only one of the tools that it can take out or tuck away at will. Also at the microscale, the wheel-within hides, for instance, in microtubules, where the ZEEM originates in the structure of the protein protofilaments making up the microtubule's lattice[56,57] or in filamentous viruses, where stresses due to attachment of sugary chains from the mucus to the virus's spike proteins induce ZEEMs.[58]

So when it comes to rivaling man-made technology, Nature's ''Mount Improbable''[1] – in the light of the wheel-within – appears as a misnomer for the epistemological blind-spot caused by our own ''Mount Incomprehensible''. In contrast to the molecular wheel–axle systems readily utilized in Nature (see the examples discussed below), the various wheels-within from Fig. 1 are kinematically difficult to comprehend at first. Yet, in spite of their intricacy, they have reemerged in different clades of life, from bacteria, plants, and insects to vertebrates at least four times independently. So the motif forms an evolutionary reachable, though not quite low-hanging, fruit, as it requires a subtle coordination/orchestration of the driving mechanism.

Hardly any example for Nature's current technological superiority stands out more than the three (sic!) distinct types of wheels integrated as parts of the bacterial flagellum machinery complex.[13,19,20] The flagellum is the spot where the classical wheel–axle and the wheel-within work in close harmony. In fact, two types of classical wheel–axle systems, mutually geared together, are coupled with a wheel-within. One of these (classic) wheels comes in many copies as an active proton driven rotary engine, while the other is a much larger, passive rotor to which the little motorized wheels cooperatively couple in order to coordinate and amplify their torque contributions.[59] Right next to them, however, is the third wheel – the bacterial flagellar hook, a wheel-within – transmitting the motions of the classical wheels around a 90° corner in a highly controlled manner to drive the rotation of the propeller unit (the flagellum). While the two classical wheels are very reminiscent of man-made technology, Nature literally ''flexes'' with its hook: When it comes to the wheel-within, there is nothing even remotely as refined as the flagellar hook. While it has been compared to an ''ideal'' or ''universal joint'',[19] unlike the hook, an ideal joint has no ability to intrinsically maintain its curved geometry. In fact, currently we have no hint on how to rebuild the full functionality of the hook's ZEEM on the macroscopic scale. Yet, extruding such a self-standing structure with an extended ZEEM along its contour would be highly beneficial. Such a hypothetical infinitely long industrially produced filament would form an ideal wheel-within, waiting to be driven in simple geometries, *via* light or other stimuli. Having a single intrinsic ZEEM would allow for a much simpler, easier to control drive than the ''ZEEM + modulator mode'' structures that have to undergo a dissipative bifurcation first. While the closed, toroidal fiberdrive seemingly solves this problem, it does so at the price of its own closure, limiting its practical flexibility and industrial scalability.

Another even more fundamental concept from Nature turning around a (this time classical) wheel–axle is the conversion of proton gradients to the synthesis of ATP in the ''ATP Synthase'' machinery of our mitochondria. The brilliant solution of coupling two fluxes (protons and ATP) that are chemically difficult to couple by utilizing the mechanics of rotation is extraordinarily elegant. The ZEEMs of a wheel-within have also the potential to couple multiple physico–chemical fluxes *via* their continuously evolving geometry. Elastic chemical engines built with elastomers, wheels and pulleys have been created in the past,[60,61] yet the dream of reproducing a mechanosynthesis similar to that achieved by ATP Synthase has not been reached so far. Wet, solvent soaked wheels-within of the future, modifying the chemical reaction rates mechanically in a cyclic manner, could open promising routes to meet the challenge. The race is on.

Author contributions

IMK and FZ conceived the ideas and co-wrote the paper.

Conflicts of interest

The authors declare no competing interests.

Data availability

This article – a review – contains all the data that we refer to in the included figures and in the cited references.

Acknowledgements

IMK acknowledges funding by ANR-DFG Grant Rodrolls. He thanks Hervé Mohrbach, Jens-Uwe Sommer, Helmut Schiessel and FZ Ulrich S. Schwarz for many fruitful discussions and constant support. The authors thank Kjetil Tofte and Vladimir M. Stojanović for their useful comments and for carefully reading the manuscript.

References

1 R. Dawkins, Why don't animals have wheels? The Sunday Times, November 24th 1996.
2 T. Ohyama, *et al.*, A multilevel multimodal circuit enhances action selection in drosophila, *Nature*, 2015, **520**, 633.
3 X. Liang, *et al.*, Mechanics of soft-body rolling motion without external torque, *Phys. Rev. Lett.*, 2025, **134**, 198401.
4 G. J. Gbur, *Falling Felines and Fundamental Physics*, Yale University Press, 2019.

5 E. J. Marey, Des mouvements que certains animaux exécutent pour retomber sur leurs pieds, lorsqu'ils sont précipités d'un lieu élevé, *C. R. Acad. Sci.*, 1894, **119**, 714.
6 T. R. Kane and M. P. Scher, A dynamical explanation of the falling cat phenomenon, *Int. J. Solids Struct.*, 1969, **5**, 663.
7 H. Essen, The cat landing on its feet revisited or angular momentum conservation and torque-free rotations of non-rigid mechanical systems, *Am. J. Phys.*, 1981, **49**, 756–758.
8 J. R. Galli, Angular momentum conservation and the cat twist, *Phys. Teach.*, 1995, **33**, 404–407.
9 Snapshots from ''ELVIS THE CROCODILE DEATH ROLL'', Australian Reptile Park, Youtube, https://youtu.be/1sqw49cQWOo, accessed Aug 11 2025.
10 Allgemeiner Deutscher Nachrichtendienst, Bild 183-33533-0005.
11 D. Agostinelli, A. Lucantonio, G. Noselli and A. DeSimone, Nutations in growing plant shoots: The role of elastic deformations due to gravity loading, *J. Mech. Phys. Solids*, 2020, **136**, 103702.
12 S. Mugnai, *et al.*, Nutation in Plants, in *Rhythms in Plants*, ed. S. Mancuso and S. Shabala, Springer, 2007.
13 S. Shibata, H. Matsunami, S.-I. Aizawa and M. Wolf, Torque transmission mechanism of the curved bacterial flagellar hook revealed by cryo-EM, *Nat. Struct. Mol. Biol.*, 2019, **26**, 941.
14 A. Bazir, A. Baumann, F. Ziebert and I. M. Kulić, Dynamics of fiberboids, *Soft Matter*, 2020, **16**, 5210.
15 A. Baumann, *et al.*, Motorizing fibres with geometric zero-energy modes, *Nat. Mater.*, 2018, **17**, 523.
16 F. E. Fish, S. A. Bostic, A. J. Nicastro and J. T. Beneski, Death roll of the alligator: mechanics of twist feeding in water, *J. Exp. Biol.*, 2007, **210**, 2811–2818.
17 N. Charon, *et al.*, The unique paradigm of spirochete motility and chemotaxis, *Annu. Rev. Microbiol.*, 2012, **66**, 349.
18 D. K. Vig and C. W. Wolgemuth, Swimming dynamics of the Lyme disease spirochete, *Phys. Rev. Lett.*, 2012, **109**, 218104.
19 F. A. Samatey, *et al.*, Structure of the bacterial flagellar hook and implication for the molecular universal joint mechanism, *Nature*, 2004, **431**, 1062–1068.
20 T. Kato, F. Makino, M. Tomoko, P. Horvath and K. Namba, Structure of the native supercoiled flagellar hook as a universal joint, *Nat. Commun.*, 2019, **10**, 5295.
21 C. Darwin, *The Power of Movement in Plants*, Appleton and Co, 1883.
22 A. Shapere and F. Wilczek, Gauge kinematics of deformable bodies, *Am. J. Phys.*, 1989, **57**, 514.
23 L. Lecornu, Sur une application du principe des aires, *C. R. Acad. Sci.*, 1894, **119**, 899–900.
24 S. Guest, E. Kebadze and S. Pellegrino, A zero-stiffness elastic shell structure, *J. Mech. Mater. Struct.*, 2011, **6**, 203–212.
25 S. Kok, G. Radaelli and A. Nobaveh, & Herder, J. Neutrally stable transition of a curved-crease planar shell structure, *Extreme Mech. Lett.*, 2021, **49**, 101469.
26 D. van der Lans, A. A. Nobaveh and G. Radaelli, Reversible shape morphing of a neutrally stable shell by untethered local activation of embedded Ni-Ti wires, *J. Intell. Mater. Syst. Struct.*, 2023, **34**, 1664.
27 M. Schenk and S. D. Guest, On zero stiffness, *Proc. Inst. Mech. Eng., Part C*, 2014, **228**, 1701–1714.
28 W. Hamouche, C. Maurini, S. Vidoli and A. Vincenti, Multi-parameter actuation of a neutrally stable shell: a flexible gear-less motor, *Proc. R. Soc. A*, 2017, **473**, 20170364.
29 Z.-Z. Nie, *et al.*, Light-driven continuous rotating möbius strip actuators, *Nat. Commun.*, 2021, **12**, 2334.
30 Q. L. Zhu, *et al.*, Closed twisted hydrogel ribbons with self-sustained motions under static light irradiation, *Adv. Mater.*, 2024, **36**, 2314152.
31 X. Yang, *et al.*, Threefold möbius machine, *Adv. Funct. Mater.*, 2025, 2420815.
32 D. Hore, A. Majumder, S. Mondal, A. Roy and A. Ghatak, How to make a cylinder roll uphill, *Soft Matter*, 2012, **8**, 5038.
33 C. Ahn, K. Li and S. Cai, Light or thermally powered autonomous rolling of an elastomer rod, *ACS Appl. Mater. Interfaces*, 2018, **10**, 25689.
34 Z. Deng, K. Li, A. Priimagi and H. Zeng, Light-steerable locomotion using zero-elastic-energy modes, *Nat. Mater.*, 2024, **23**, 1728–1735.
35 J.-C. Choi, *et al.*, Steerable and agile light-fueled rolling locomotors by curvature-engineered torsional torque, *Adv. Sci.*, 2023, **10**, 2304715.
36 Q. Liu, *et al.*, Dynamic liquid crystal elastomers for body heat- and sunlight-driven self-sustaining motion via material-structure synergy, *Angew. Chem., Int. Ed.*, 2025, **64**, e202500527.
37 Q. L. Zhu, *et al.*, Animating hydrogel knotbots with topology-invoked self-regulation, *Nat. Commun.*, 2024, **15**, 300.
38 P. Yang, *et al.*, Motorizing the buckled blister for rotary actuation, *Exploration*, 2024, **4**, 20230055.
39 T. Zang, *et al.*, Self-sustained liquid crystal elastomer actuators with geometric zero-elastic-energy modes, *Macromol. Rapid Commun.*, 2025, 2500134.
40 C. Chen, *et al.*, Advancing physical intelligence for autonomous soft robots, *Sci. Robot.*, 2025, **10**, eads1292.
41 F. Qi, *et al.*, Defected twisted ring topology for autonomous periodic flip-spin-orbit soft robot, *Proc. Natl. Acad. Sci. U. S. A.*, 2024, **121**, e2312680121.
42 W. Ai, J. Wu, Y. Long and K. Song, A rolling light-driven pneumatic soft actuator based on liquid-gas phase change, *Adv. Mater.*, 2025, 2418218.
43 S. Mondal and A. Ghatak, Rolling of an elastomeric cylinder: A marangoni like effect in solid, *Extreme Mech. Lett.*, 2015, **3**, 24.
44 Y. Yu, C. Du, K. Li and S. Cai, Controllable and versatile self-motivated motion of a fiber on a hot surface, *Extreme Mech. Lett.*, 2022, **57**, 101918.
45 Y. Yu, *et al.*, Lightdriven core-shell fiber actuator based on carbon nanotubes/liquid crystal elastomer for artificial muscle and phototropic locomotion, *Carbon*, 2022, **187**, 97.
46 X. Zhou, *et al.*, Multimodal autonomous locomotion of liquid crystal elastomer soft robot, *Adv. Sci.*, 2024, **11**, 2402358.

47 Z.-C. Jiang, Y.-Y. Xiao, R.-D. Cheng, J.-B. Hou and Y. Zhao, Dynamic liquid crystalline networks for twisted fiber and spring actuators capable of fast light-driven movement with enhanced environment adaptability, *Chem. Mater.*, 2021, **33**, 6541.
48 Y. Zhao, *et al.*, Physically intelligent autonomous soft robotic maze escaper, *Sci. Adv.*, 2023, **9**, eadi3254.
49 Z.-Z. Nie, M. Wang, S. Huang, Z.-Y. Liu and H. Yang, Multimodal self-sustainable autonomous locomotions of light-driven seifert ribbon actuators based on liquid crystal elastomers, *Angew. Chem., Int. Ed.*, 2023, **62**, e202304081.
50 Ed. Pellegrino, S., Guest, S. D. and Gladwell, G. M. L., *IUTAM-IASS Symposium on Deployable Structures, vol. 80 of Solid Mechanics and Its Applications*, Springer Netherlands, Dordrecht, 2000.
51 K. A. Seffen and S. D. Guest, Prestressed Morphing Bistable and Neutrally Stable Shells, *J. Appl. Mech.*, 2011, **78**, 011002.
52 C. Vehar, S. Kota and R. Dennis, Closed-Loop Tape Springs as Fully Compliant Mechanisms, in Vol. 2*: 28th Biennial Mechanisms and Robotics Conference*, 1023–1032 (ASMEDC, Salt Lake City, Utah, USA, 2004).
53 D. Forster, *Hydrodynamic Fluctuations, Broken Symmetry, and Correlation Functions*, CRC Press, 2018.
54 P. Chaikin and T. C. Lubensky, *Principles of Condensed Matter Physics*, Cambridge University Press, 1995.
55 B. C. Jayne, What Defines Different Modes of Snake Locomotion?, *Integr. Comp. Biol.*, 2020, **60**, 156–170.
56 H. Mohrbach, A. Johner and I. Kulić, Tubulin bistability and polymorphic dynamics of microtubules, *Phys. Rev. Lett.*, 2010, **105**, 268102.
57 F. Ziebert, H. Mohrbach and I. Kulić, Why microtubules run in circles - mechanical hysteresis of the tubulin lattice, *Phys. Rev. Lett.*, 2015, **114**, 147101.
58 F. Ziebert, K. G. Dokonon and I. M. Kulić, Reshaping and enzymatic activity may allow viruses to move through the mucus, *Soft Matter*, 2024, **20**, 7185.
59 N. Wadhwa and H. C. Berg, Bacterial motility: machinery and mechanisms, *Nat. Rev. Microbiol.*, 2022, **20**, 161.
60 I. Z. Steinberg, A. Oplatka and A. Katchalsky, Mechanochemical Engines, *Nature*, 1966, **210**, 568–571.
61 E. Pines, K. L. Wun and W. Prins, Mechanochemical energy conversion, *J. Chem. Educ.*, 1973, **50**, 753.